Protein Cell 2011, 2(5): 410–422
DOI 10.1007/s13238-011-1049-7

Protein & Cell

RESEARCH ARTICLE

Targeted deletion of mouse *Rad1* leads to deficient cellular DNA damage responses

Chunbo Zhang[1,2,4*], Yuheng Liu[1,3*], Zhishang Hu[1], Lili An[1], Yikun He[2], Haiying Hang[1] ✉

[1] National Laboratory of Biomacromolecules, and the Center for Computational and Systems Biology, Institute of Biophysics, Chinese Academy of Sciences, Beijing 100101, China
[2] College of Life Science, Capital Normal University, Beijing 100037, China
[3] Graduate School of the Chinese Academy of Sciences, Beijing 100049, China
[4] Current address: School of Pharmacy, Faculty of Medicine, The Chinese University of Hong Kong, Shatin, Hong Kong, China
✉ Correspondence: hh91@sun5.ibp.ac.cn
Received April 23, 2011 Accepted May 5, 2011

ABSTRACT

The *Rad1* gene is evolutionarily conserved from yeast to human. The fission yeast *Schizosaccharomyces pombe* *Rad1* ortholog promotes cell survival against DNA damage and is required for G_2/M checkpoint activation. In this study, mouse embryonic stem (ES) cells with a targeted deletion of *Mrad1*, the mouse ortholog of this gene, were created to evaluate its function in mammalian cells. *Mrad1*$^{-/-}$ ES cells were highly sensitive to ultraviolet-light (UV light), hydroxyurea (HU) and gamma rays, and were defective in G_2/M as well as S/M checkpoints. These data indicate that *Mrad1* is required for repairing DNA lesions induced by UV-light, HU and gamma rays, and for mediating G_2/M and S/M checkpoint controls. We further demonstrated that *Mrad1* plays an important role in homologous recombination repair (HRR) in ES cells, but a minor HRR role in differentiated mouse cells.

KEYWORDS Rad1, DNA damage, checkpoint signaling, DNA repair, homologous recombination repair

INTRODUCTION

Cells face endogenous and exogenous assaults that damage genomic DNA. But eukaryotic cells have conserved surveillance mechanisms, which could detect the DNA lesions and send the signals to the DNA repair system and the cell cycle control machinery, to coordinate DNA repair and minimize negative effects of these lesions. The cell cycle delay induced via the checkpoint mechanism is thought to provide extra time for DNA damage repair, and to prevent cell cycle progression into critical phases that could lead to lethality (Hartwell and Weinert, 1989; Paulovich and Hartwell, 1995; Zhou et al., 2010).

Rad9, *Rad1* and *Hus1* are a group of genes conserved from yeast to human that play key roles in the cell cycle signaling networks. Their protein products form a ring-shaped heterotrimer, named the 9-1-1 complex (Doré et al., 2009; Sohn and Cho, 2009; Xu et al., 2009). It is believed that this complex is important for the functions of DNA repair as well as the activation of cell cycle checkpoints (Shiomi et al., 2002; Bermudez et al., 2003; Ellison and Stillman, 2003). Interestingly, human Rad1 (i.e., RAD1) also exists as monomer besides forming the 9-1-1 complex in cells, and the function of this form of the protein is unknown (Burtelow et al., 2001). In fission yeast *Schizosaccharomyces pombe*, disruption mutants of the three genes resulted in similar phenotypes, including viability, sensitivity to UV-light, the replication inhibitor hydroxyurea (HU), as well as gamma rays, and defective S/M and G_2/M checkpoint control (al-Khodairy and Carr, 1992; Enoch et al., 1992; Lieberman et al., 1992; Murray et al., 1991; Rowley et al., 1992). Disruption of the budding yeast *Saccharomyces cerevisiae* counterparts, *Mec3* (*schus1*), *Rad17* (*scrad1*) and *Ddc1* (*scrad9*), also caused similar phenotypes in the corresponding mutants, including hypersensitivity to UV light, HU and gamma rays, and G_2/M checkpoint defect, but not a disruption of the S/M checkpoint defect (Longhese et al., 1997; Lydall and Weinert, 1997). Mouse cells with a disruption of *Mrad9* or *Mhus1*, the mouse homologues of *rad9* or *hus1*, were successfully created, and also exhibited significantly higher sensitivity to UV light, HU and gamma rays than the wild-type cells (Weiss et al., 2000;

[*]These authors contributed equally to the work.

 © Higher Education Press and Springer-Verlag Berlin Heidelberg 2011

Hopkins et al., 2004). The cell cycle checkpoint functions of *Mrad9* and *Mhus1* were reported to be different but the comparison was based on the data using two different cell types (Weiss et al., 2000; Hopkins et al., 2004; Wang et al., 2004). The *Mhus1*$^{-/-}$ cells are mouse embryonic fibroblasts (MEF), while the *Mrad9*$^{-/-}$ cells are mouse embryonic stem cells (ES). *Mhus1*$^{-/-}$ MEFs were defective in the UV light-induced intra-S phase checkpoint, but functioned normally with respect to the G_2/M checkpoint (Weiss et al., 2003). In contrast, *Mrad9*$^{-/-}$ ES cells were not markedly defective in the UV light-induced intra-S phase checkpoint, but failed to maintain G_2/M checkpoint control following the exposure to gamma rays (Weiss et al., 2000; Hopkins et al., 2004).

Results from human *RAD1* knockdown using siRNA suggested that the gene is an important element for cell growth and is required for the recovery of DNA synthesis following HU treatment (Bao et al., 2004). The same study showed that reduced RAD1 protein level caused a defect in the intra-S phase checkpoint but did not affect the G_2/M checkpoint. However, *rad1*-disrupted yeast cells failed to arrest in response to ionizing radiation exposure (al-Khodairy and Carr, 1992; Enoch et al., 1992; Rowley et al., 1992; Lydall and Weinert, 1997).

Although targeted deletion of *Mrad9* and *Mhus1* in mouse cells and mice have been reported (Weiss et al., 2000; Hopkins et al., 2004; Levitt et al., 2005; Levitt et al., 2007; Hu et al., 2008; Yazinski et al., 2009; An et al., 2010), equivalent studies for *Mrad1* have not been published. Such investigation is important to reveal the gene functions that are not detectable when RAD1 protein is only partially expressed in siRNA knockdown cells (Bao et al., 2004) or heterozygous cells (Han et al., 2010). In the present study, we constructed mouse ES cells with a targeted deletion of *Mrad1* gene and investigated *Mrad1* function in these cells. Our results showed that *Mrad1* homozygously deleted ES cells were viable, but were defective in G_2/M checkpoint maintenance as well as the HU-induced S/M checkpoint, and were highly sensitive to UV light, HU and gamma rays. Interestingly, the differentiation of *Mrad1*$^{-/-}$ ES cells modulated the capability of double-strand breaks (DSB) repair.

RESULTS

Construction of mouse ES cells with homozygous disruptions of *Mrad1*

Mrad1$^{+/-}$ ES cells were obtained as previously described (Han et al., 2010). The *neo* gene product can destroy antibiotic G418, and the *Mrad1*$^{+/-}$ ES cells contained one allele of disrupted genomic *Mrad1* bearing a copy of *neo* gene. We hypothesize that increasing G418 concentration in the medium might force the amplification of the copy number of *neo* and even replace the remaining wild type genomic *Mrad1* with the *neo*-bearing disrupted genomic *Mrad1.* To obtain *Mrad1*$^{-/-}$ clones, the *Mrad1*$^{+/-}$ ES cells were incubated with 3.2–4.4 mg/mL G418 instead of the original 300 µg/mL G418 for 20 days, and from 96 survivors, six colonies bearing *Mrad1* homozygous deletion were identified by Southern blotting (Fig. 1A). These results were confirmed using Northern blotting (Fig. 1B) and RT-PCR (Fig. 1C).

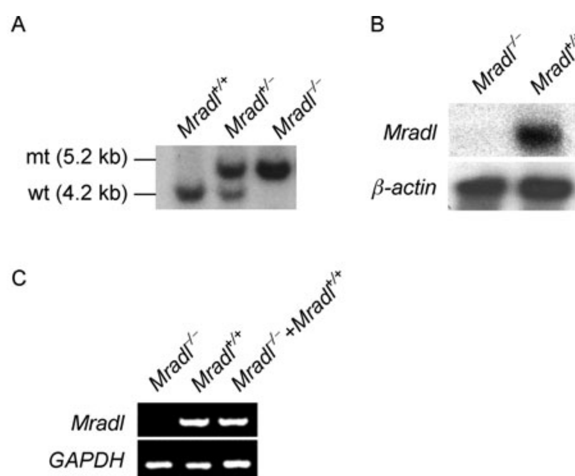

Figure 1. Targeted deletion of mouse *Mrad1*. (A) Southern blot of *Mrad1* in mouse ES cells. Genomic DNA from wild-type and targeted ES clones were digested with *Hin*dIII and hybridized with probes corresponding to flanking sequences. Bands indicate wild-type and deleted *Mrad1* alleles. (B) Northern blot of *Mrad1* RNA in mouse ES cells. The β-actin gene was used as a control to demonstrate equivalent sample loading. The probe for *Mrad1* RNA was made from the digested sequence of genomic *Mrad1* gene. (C) RT-PCR to assess *Mrad1* RNA levels. Total RNA was isolated from *Mrad1*$^{+/+}$ and *Mrad1*$^{-/-}$ ES cells, the latter ectopically expressing *Mrad1*. *Gapdh* RNA levels were used as an internal control. Primer pairs and other experimental details are described in MATERIALS AND METHODS.

Mrad1 deletion retards cell proliferation and alters cell cycle phase distribution

RAD1 knockdown by siRNA reduced the proliferation rate of human cells (Bao et al., 2004). Consistent with this result, *Mrad1*$^{-/-}$ ES cells grew significantly slower than the wild type control population (Fig. 2A), and formed much smaller colonies (Fig. 2B). We examined the cell cycle phase distributions of *Mrad1*$^{-/-}$ and *Mrad1*$^{+/+}$ cells with flow cytometry, and found that significantly more *Mrad1*$^{-/-}$ cells accumulated in the G_2/M phase than the wild-type cells (Fig. 2C), suggesting the mutant cells proceeded through G_2/M at a significantly slower pace. Bromodeoxyuridine (BrdU) incorporation analysis showed that S phase progression rate was reduced by homozygous deletion of *Mrad1* (Fig. 2D). All the aforementioned changes in the cell cycle caused by *Mrad1* deletion were reversed by ectopically expressing

© Higher Education Press and Springer-Verlag Berlin Heidelberg 2011

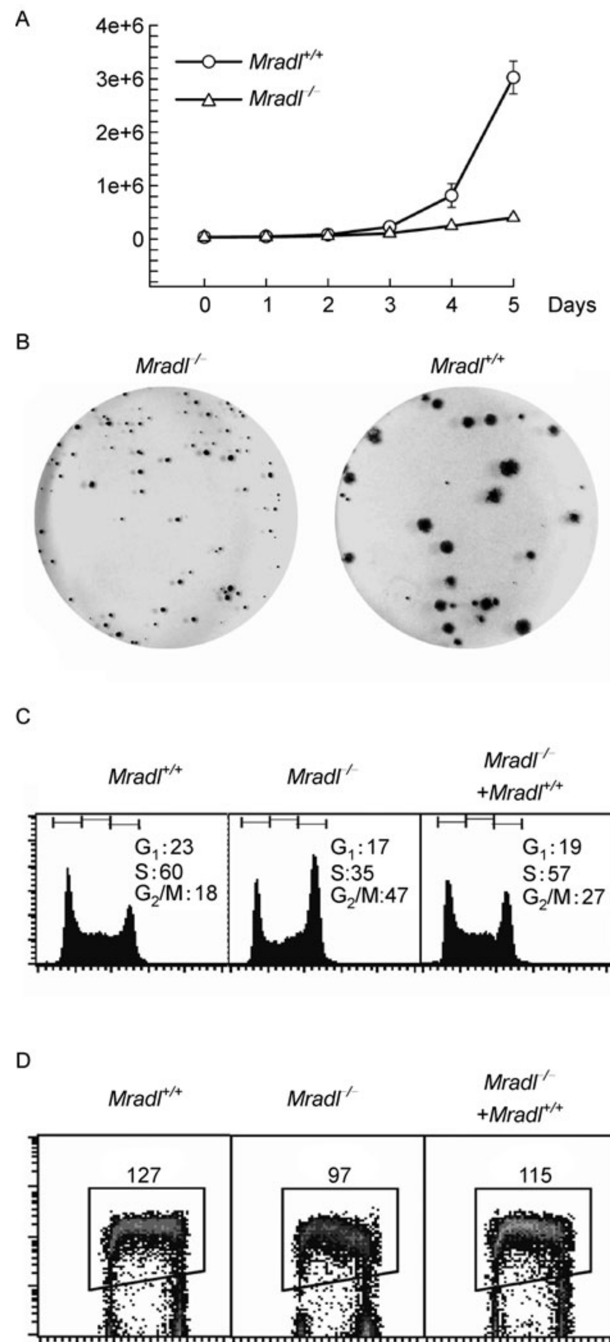

Figure 2. Deletion of *Mrad1* in mouse ES cells retards cell proliferation and changes cell cycle phase distribution. (A) Proliferation of *Mrad1*$^{+/+}$ and *Mrad1*$^{-/-}$ ES. The average results were derived from three independent experiments. (B) Cells were grown on Petri dishes at 37°C with 5% CO_2 for 10 days and then stained to visualize colony formation. *Mrad1*$^{-/-}$ ES cells (left) formed much smaller colonies than *Mrad1*$^{+/+}$ ES cells (right). (C) Asynchronously dividing ES cells were fixed and stained with PI. Cell cycle distribution was analyzed by flow cytometry. Deletion of *Mrad1* resulted in an aberrant accumulation of cells in the G_2/M phase, suggesting a slower progression through this phase of cell cycle. The percentage of each cell population in G_1, S and G_2/M phases is shown in the graphs as indicated. (D) S-phase DNA replication was assayed by simultaneous measurement of DNA content and BrdU incorporation. Deletion of *Mrad1* resulted in a slowdown of S phase DNA synthesis. The number inside each graph is the geometric mean of BrdU incorporation per 10 min. All the above experiments had been repeated at least three times. Only one set of representative data was presented here.

 © Higher Education Press and Springer-Verlag Berlin Heidelberg 2011

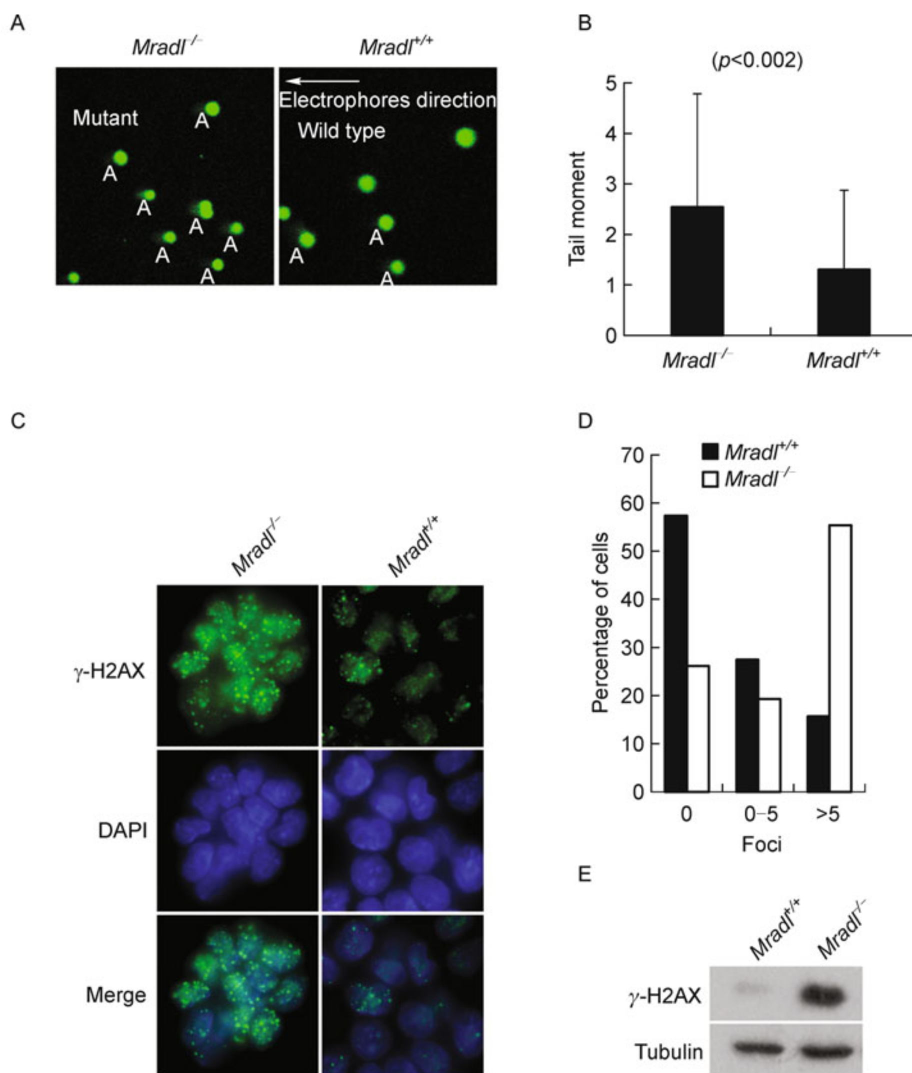

Figure 3. Deletion of *Mrad1* leads to increased frequency of DNA lesions. (A) *Mrad1*$^{-/-}$ and *Mrad1*$^{+/+}$ ES cells were analyzed for DNA lesions using a Comet Assay kit as described in MATERIALS AND METHODS. (B) The tail moment of *Mrad1*$^{-/-}$ ES cells was measured and the mean ± SD is depicted. The tail moment of the mutant cells was significantly larger than wild-type control ($p < 0.002$). (C) Spontaneous DNA double-strand breaks were detected by γ-H2AX labeling. (D) Quantitative assessments were made by counting foci in at least 100 cells of each phenotype, and the percentage of foci containing cells is shown. (E) Whole cell lysates from *Mrad1*$^{+/+}$ *and Mrad1*$^{-/-}$ ES cells were subjected to western blotting using anti-γ-H2AX antibody, with tubulin served as a loading control.

Mrad1 (Fig. 2C and 2D; data not shown), and thus these alterations were due to the lack of *Mrad1* function.

The increased accumulation of *Mrad1*$^{-/-}$ cells in the G_2/M phase might result from activation of the G_2/M checkpoint by DNA lesions, and therefore, we monitored the DNA breaks in wild type and *Mrad1*$^{-/-}$ ES cells using an alkaline comet assay for all types of DNA lesions and a histone γ-H2AX assay for DSBs. The comet tail moment in *Mrad1*$^{-/-}$ ES cells was significantly higher than that in *Mrad1*$^{+/+}$ cells (Fig. 3A and 3B), indicating the presence of more DNA lesions in the mutant. These results were confirmed by the histone γ-H2AX assay, in which more foci (Fig. 3C and 3D) as well as a higher level of histone γ-H2AX were detected in the mutant population (Fig. 3E), reflecting enhanced DNA DSBs in *Mrad1*$^{-/-}$ ES cells.

Failure of *Mrad1*$^{-/-}$ ES cells to maintain ionizing radiation-induced G_2/M checkpoint control

DNA damage-induced arrest in G_2 phase is one of the most prominent cell cycle checkpoints in eukaryotic cells. Fission yeast *S. pombe rad1* is required for this cell cycle arrest in

© Higher Education Press and Springer-Verlag Berlin Heidelberg 2011

response to ionizing radiation exposure (Freire et al., 1998; Udell et al., 1998). Therefore, we examined whether the role of *Mrad1* in the G_2/M checkpoint is evolutionarily conserved. *Mrad1*$^{+/+}$ and *Mrad1*$^{-/-}$ cells, as well as the *Mrad1*$^{-/-}$ cells ectopically expressing *Mrad1* were irradiated with 10 Gy of gamma rays, harvested at 4, 6, 8, 10 and 12 h after exposure, and then processed for flow cytometric analysis to assess cell cycle phase distribution. Only data from untreated, 6 and 10 h time points are presented here because the rest of data essentially indicated the same trends. The percentage of cell populations in each phase of the cell cycle is shown in graphic (Fig. 4) and tabular formats (Table 1). Subpopulations of both *Mrad1*$^{+/+}$ and *Mrad1*$^{-/-}$ ES cells increased in the G_2/M phase and decreased in the G_1 and S phases post irradiation. This pattern, lacking G_1 arrest but exhibiting radiation-inducible G_2 arrest, is a typical response of wild-type ES cells to gamma rays (Aladjem et al., 1998). This result indicated that *Mrad1* is not indispensable to activate the G_2/M checkpoint. However, in contrast to the wild-type cells, *Mrad1*-deficient cells accumulated in the G_1 phase (arrows in Fig. 4). To assess whether the small G_1 subpopulation of cells came from the G_2/M phase post irradiation, colcemid, which disrupts the mitotic spindle and traps cells in mitosis, was added to the cells. The results showed that incubation of the cells with colcemid eliminated the small G_1 subpopulation accumulation, and therefore the cells progressed from the G_2/M phase (Fig. 4), suggesting the important role of *Mrad1* in maintaining the DNA damage-induced G_2/M checkpoint control. This conclusion was confirmed by the fact that the G_2/M checkpoint defect was rescued by the ectopic expression of *Mrad1*.

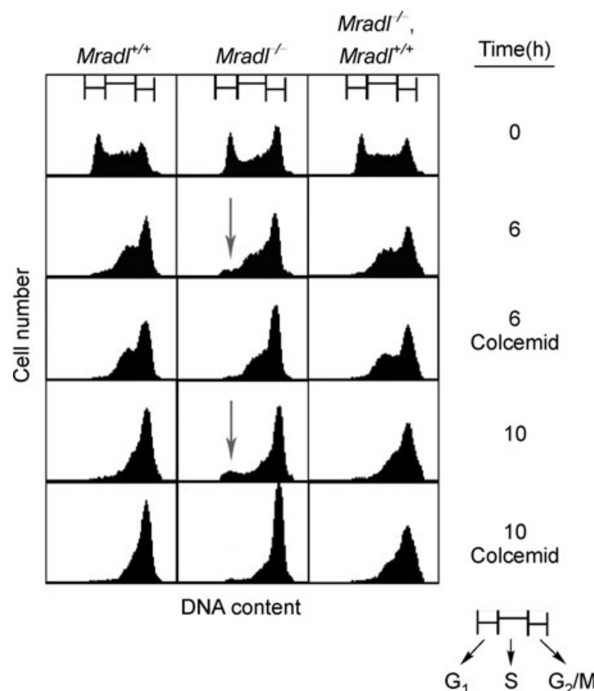

Figure 4. *Mrad1* deletion leads to a deficiency in G_2 arrest induced by ionizing radiation exposure. *Mrad1*$^{+/+}$, *Mrad1*$^{-/-}$ ES cells, and *Mrad1*$^{-/-}$ ES cells ectopically expressing *Mrad1* were mock-treated or treated with 10 Gy of gamma rays in the absence or presence of colcemid, and then analyzed by flow cytometry. G_1, S and G_2/M regions of the profiles are delineated on top of graph for the calculations of cell distribution in each phase as indicated in Table 1.

Table 1 Percentage of cells in different phases of the cell cycle at indicated times post-irradiation with 10 Gy of gamma rays

Genotype	Post-irradiation time (h)	Percentage of population in all cycle phase (%)		
		G_1	S	G_2/M
	0	22.27	48.43	24.55
	6	1.56	45.14	52.95
Mrad1$^{+/+}$	6 + colcemid	0.64	43.18	56.05
	10	0.79	27.01	71.04
	10 + colcemid	0.38	23.01	76.26
	0	24.07	35.41	40.51
	6	5.73	42.85	51.18
Mrad1$^{-/-}$	6 + colcemid	1.22	37.50	61.11
	10	9.02	24.90	65.29
	10 + colcemid	0.73	14.56	83.70
	0	23.58	44.94	31.36
	6	1.15	46.86	50.40
Mrad1$^{-/-}$ + *Mrad1*$^{+/+}$	6 + colcemid	0.59	42.90	55.25
	10	1.13	32.94	63.04
	10 + colcemid	0.44	30.35	66.40

 © Higher Education Press and Springer-Verlag Berlin Heidelberg 2011

Mrad1 disruption in ES cells alters S/M checkpoint control

S. pombe rad1 is required to block cells with incomplete DNA replication from moving into the M phase of cell cycle (S/M checkpoint), while the *S. cerevisiae* ortholog, *Rad17* (*scRad1*), is dispensable for the checkpoint. To determine whether the S/M checkpoint in mouse ES cells is *Mrad1*-dependent, we examined the level of phospho-histone-H3 (γ-H3) throughout the cell cycle. Histone-H3 is specifically phosphorylated during mitosis. After treatment with HU for different times, ES cells were labeled with anti-γ-H3 antibody, stained with propidium iodide (PI) for DNA content, and then analyzed by flow cytometry. Incubation with HU reduced the number of γ-H3 positive *Mrad1*$^{+/+}$ cells with 2N DNA content because most cells were blocked in S phase and thus fewer moved into the M phase. Few *Mrad1*$^{+/+}$ cells with less than 2N DNA content were γ-H3 positive after HU treatment, indicating that the wild type cells have a normal S/M checkpoint (Fig. 5 and Table 2). In contrast, the number of γ-H3 positive *Mrad1*$^{-/-}$ cells with less than 2N DNA content dramatically increased after HU treatment. *Mrad1*-deficient ES cells ectopically expressing *Mrad1* showed the same pattern as wild-type cells. Therefore, *Mrad1* is essential for the S/M checkpoint control.

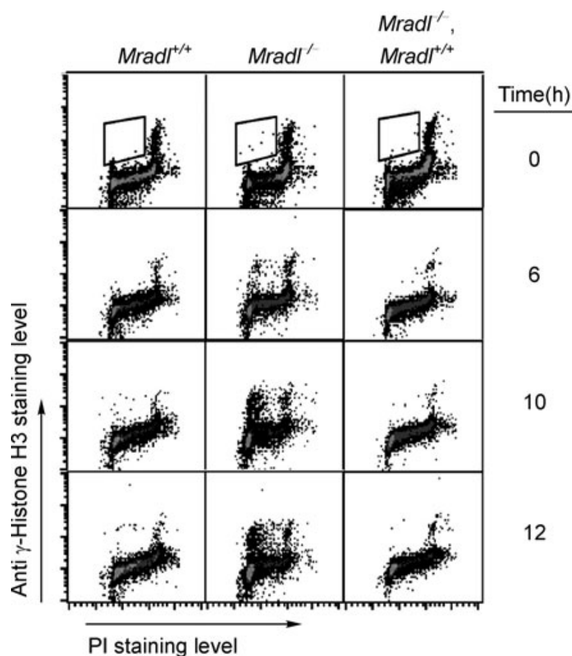

Figure 5. *Mrad1* deletion leads to an S/M checkpoint control defect. *Mrad1*$^{+/+}$, *Mrad1*$^{-/-}$ ES cells, and *Mrad1*$^{-/-}$ ES cells ectopically expressing *Mrad1* were treated or mock-treated with 1 mmol/L HU for various times. Cells were collected and labeled with antibodies against the mitotic marker phosphor-histone H3, stained with PI, and analyzed by flow cytometry. Staining intensity for PI (*x*-axis) is plotted *versus* staining intensity of phosphor-histone H3 (*y*-axis). Cells in the boxed region correspond to the prematurely condensed chromosome mitotic fraction. The percentage of boxed cells in the graphs is listed in Table 2.

Table 2 Percentage of cells with premature condensed chromosomes (phosphor-histone H3 labeled cells with less than 2N DNA) treated for indicated times with 1 mmol/L HU

Genotype	Treatment time (h)	Percentage of γ-H3 positive with less than 2N DNA (%)
Mrad1$^{+/+}$	0	0.03
	6	0.04
	10	0.12
	12	0.24
Mrad1$^{-/-}$	0	0.07
	6	0.83
	10	4.88
	12	6.04
Mrad1$^{-/-}$ + *Mrad1*$^{+/+}$	0	0.01
	6	0.02
	10	0.04
	12	0.05

Mrad1 is not essential for the intra-S phase checkpoint induced by UV light

The intra-S phase cell cycle checkpoint monitors DNA replication and delays DNA synthesis in the presence of DNA damage. We demonstrated that *Mrad1*-null cells are highly sensitive to UV light (see below). Therefore, we determined whether the UV-induced intra-S phase checkpoint of the mutant cells was aberrant. *Mrad1*$^{+/+}$ and *Mrad1*$^{-/-}$ cells were treated with UV light, and then pulse-labeled with 10 μmol/L BrdU at designated times post treatment to detect DNA replication by flow cytometry. The incorporation rates of BrdU into DNA in both cell populations dramatically reduced at 40, 90 and 180 min after irradiation, and the kinetics were similar (Fig. 6). Thus, these findings indicate that deletion of *Mrad1* does not affect the intra-S phase checkpoint control after exposure to UV light.

Mrad1-deleted ES cells are hypersensitive to UV light, HU and gamma rays

Previous research showed that Rad1 associates with Hus1 and Rad9 in a 9-1-1 heterotrimer to respond to DNA damage (Hang and Lieberman, 2000; Rauen et al., 2000; Lindsey-Boltz et al., 2001; Roos-Mattjus et al., 2002; Parrilla-Castellar et al., 2004). Both *Mhus1*$^{-/-}$ MEF cells and *Mrad9*$^{-/-}$ mouse ES cells are highly sensitive to genotoxins, including UV light, HU and gamma rays (Weiss et al., 2000; Hopkins et al., 2004; Wang et al., 2004; Wang et al., 2006). *S. pombe rad1::ura4*$^{+}$

© Higher Education Press and Springer-Verlag Berlin Heidelberg 2011

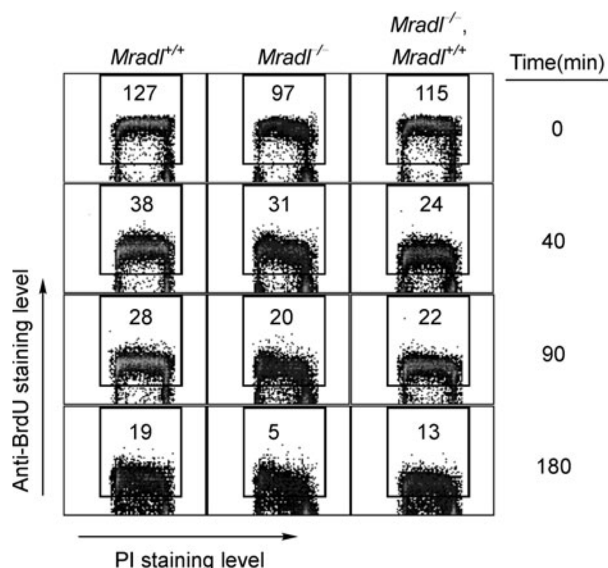

Figure 6. ***Mrad1*-deficient ES cells demonstrate a normal delay in DNA synthesis in response to UV light exposure.** *Mrad1*$^{+/+}$, *Mrad1*$^{-/-}$ ES cells, and *Mrad1*$^{-/-}$ ES cells ectopically expressing *Mrad1* were treated or mock-treated with 20 J/m^2 UV, labeled with BrdU at the indicated times post exposure, stained with FITC-conjugated anti-BrdU antibody and PI, and then analyzed by flow cytometry. Staining intensity for PI (*x*-axis) *versus* staining intensity for BrdU (*y*-axis) is indicated. Geometric means of the FITC fluorescence in BrdU-positive cells, which reflects the BrdU uptake rate by the S phase subpopulation of cells, are shown in each sample.

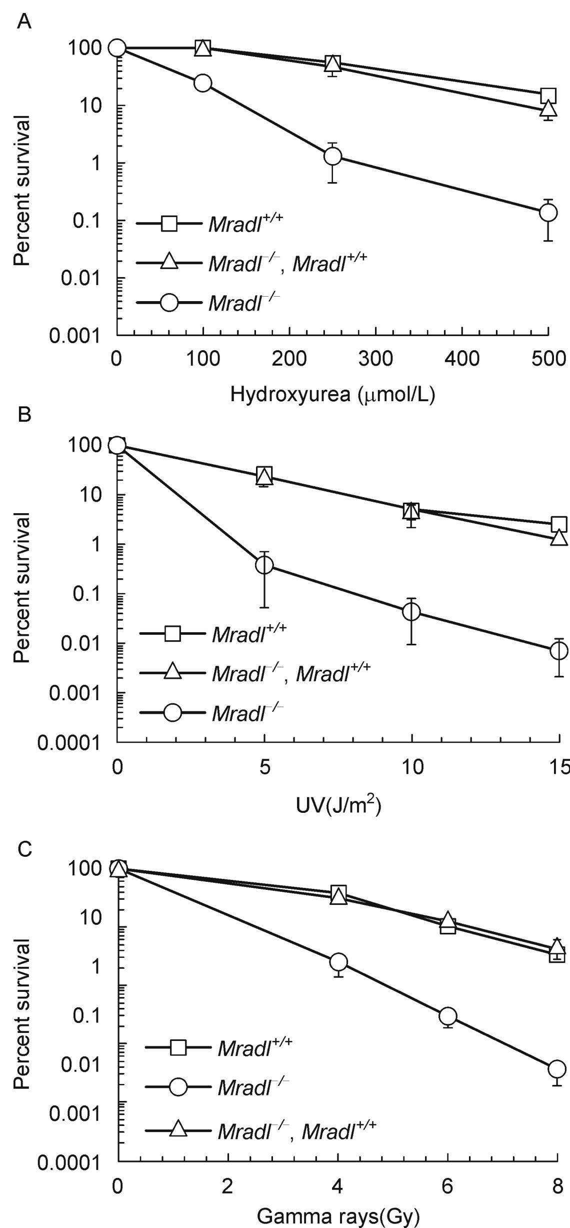

Figure 7. ***Mrad1*-deficient cells have increased sensitivity to DNA-damaging agents.** *Mrad1*$^{+/+}$, *Mrad1*$^{-/-}$ ES cells, and *Mrad1*$^{-/-}$ ES cells ectopically expressing *Mrad1* were treated as described in MATERIALS AND METHODS, and colony formation was used to assess their sensitivity to hydroxyurea (A), UV (B), and gamma rays (C). Points in all the graphs represented the average of three independent experiments, with bars indicating standard deviation.

cells are also extremely sensitive to these DNA damaging agents (Freire et al., 1998; Udell et al., 1998). Therefore, we examined whether Rad1 in mouse ES cells plays an important role in promoting resistance to these genotoxins. As shown in Fig. 7, *Mrad1*$^{-/-}$ ES cells were extremely sensitive to UV light, HU and gamma rays compared to the wild type control population. To confirm the sensitivities are due to a defect in *Mrad1*, resistance was examined in the mutant cells ectopically expressing the wild-type gene. As indicated in Fig. 7, expression of wild-type *Mrad1* compensated the resistance to UV light, HU and gamma rays in *Mrad1*$^{-/-}$ ES cells, thus indicating that *Mrad1* gene mediates the resistance to these agents.

Deletion of *Mrad1* does not affect expression of other cell cycle checkpoint genes

p21, *p53*, *Hus1* and *Rad9* are important cell cycle checkpoint genes, and the expression levels of *p21*, *p53*, *Hus1 and Rad9* were examined by northern blotting to gain a mechanistic insight into the potential influence of *Mrad1* deletion on the regulation of these genes. The results indicated that homozygous deletion of *Mrad1* did not affect expression of these cell cycle checkpoint genes (Fig. 8). *Mrad1*$^{-/-}$ cells bearing the *Mrad1* cDNA also displayed similar expression levels of these cell cycle checkpoint RNAs, except for the increased expression of *Mhus1*, and the deletion of *Mrad1* did not affect *Mhus1* RNA level. Therefore, *Mrad1* deletion did not cause a dramatic shift in RNA levels corresponding to this group of cell cycle checkpoint genes, suggesting that the deletion caused

 © Higher Education Press and Springer-Verlag Berlin Heidelberg 2011

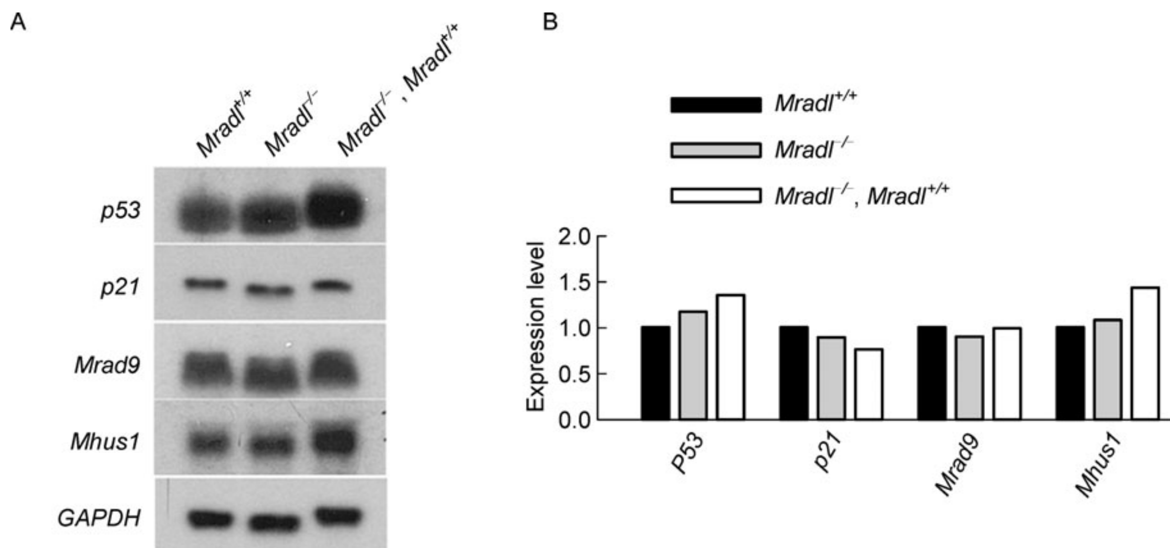

Figure 8. Northern blotting analyses of cell cycle checkpoint genes in mouse ES cells. (A) Total RNA prepared from ***Mrad1***$^{+/+}$, *Mrad1*$^{-/-}$ ES cells, and *Mrad1*$^{-/-}$ ES cells ectopically expressing *Mrad1* was subjected to Northern blotting hybridization with indicated ^{32}P-labeled cDNA probes. *Gapdh* served as a loading control. (B) Quantitative analysis of RNA levels corresponding to the checkpoint control genes. The ratio of radioactive intensity of indicated gene over *Gapdh* levels in (A) was quantified with AlphaEaseFC^{TM} software (AlphaImager 2200, Alpha Innotech Corp., San Leandro, CA).

defects of cell checkpoints and altered cell cycle distribution not through regulating the expression of *p21*, *p53*, *Hus1* or *Rad9*.

Differentiated *Mrad1*-deleted ES cells have more efficient HR repair

It has been reported that ES cells have more efficient DNA repair than differentiated ES cells in response to various DNA-damage agents (Maynard et al., 2008; Tichy and Stambrook, 2008). However, in the cell survival assay, we found that *Mrad1*$^{-/-}$ ES cells were hypersensitive to IR, but retinoic acid (RA)-induced differentiated *Mrad1*$^{-/-}$ ES cells had nearly identical sensitivity as the wild type cells (Fig. 9A). Meanwhile, undifferentiated and differentiated *Mrad1*$^{+/+}$ ES cells displayed similar resistance to the same doses of irradiation (Fig. 9B). Leukemia inhibitory factor (LIF) is routinely added to ES cell medium to prevent ES cells from differentiation. Here we obtained similar results when *Mrad1*$^{-/-}$ ES cells were cultured in RA-containing medium as well as LIF-free medium (Fig. 9C), confirming that mouse ES cell differentiation compensated for DNA repair defects caused by *Mrad1* deletion. Treatment by gamma rays causes DSBs, which are repaired by two major pathways, non-homologous end joining (NHEJ) and homologous recombination (HR). Using an established *in vivo* HR assay (Pierce et al., 2001), we found that the loss of *Mrad1* caused significant reduction in HR repair capacity, but differentiation could largely compensate it in *Mrad1*$^{-/-}$ ES cells (Fig. 9D and 9E).

DISCUSSION

In fission yeast *S. pombe*, *rad1* is a key component that mediates multiple cellular responses to DNA damage, including a role in cell cycle checkpoint (Murray et al., 1991; al-Khodairy and Carr, 1992; Enoch et al., 1992; Lieberman et al., 1992; Rowley et al., 1992; Parker et al., 1998). However, the function of this gene in mammals is not clear. In this report, we examined the activities of *Mrad1*, the mouse ortholog of *S. pombeRad1*, by creating and characterizing the mouse ES cells with deletion of *Mrad1*. We demonstrated that *Mrad1*-deficient ES cells were highly sensitive to UV light, HU and gamma rays (Fig. 7), defective in S/M and G_2/M cell cycle checkpoint controls (Fig. 4–6), and prone to accumulate DNA lesions under normal growth conditions (Fig. 3). These data indicate that *Mrad1* plays essential roles in the resistance to UV light, HU and gamma rays, as well as in the S/M and G_2/M checkpoints.

As shown by previous reports (Burtelow et al., 2001; Roos-Mattjus et al., 2002), as well as 9-1-1 complex crystal structure (Doré et al., 2009; Sohn and Cho, 2009; Xu et al., 2009), Rad1 along with Rad9 and Hus1 in a trimeric checkpoint complex were believed to have similar functions. Indeed as we showed above, many phenotypes such as the hypersensitivity to HU, UV light and gamma rays are similar among *Mrad1*-deletion, *Mrad9*-deletion and *Mhus1*-deletion mouse cells (Fig. 7) (Weiss et al., 2000, 2003; Hopkins et al., 2004). In addition, mouse ES cells with *Mrad1*-deletion and *Mrad9*-deletion are similarly deficient in G_2/M and S/M

© Higher Education Press and Springer-Verlag Berlin Heidelberg 2011

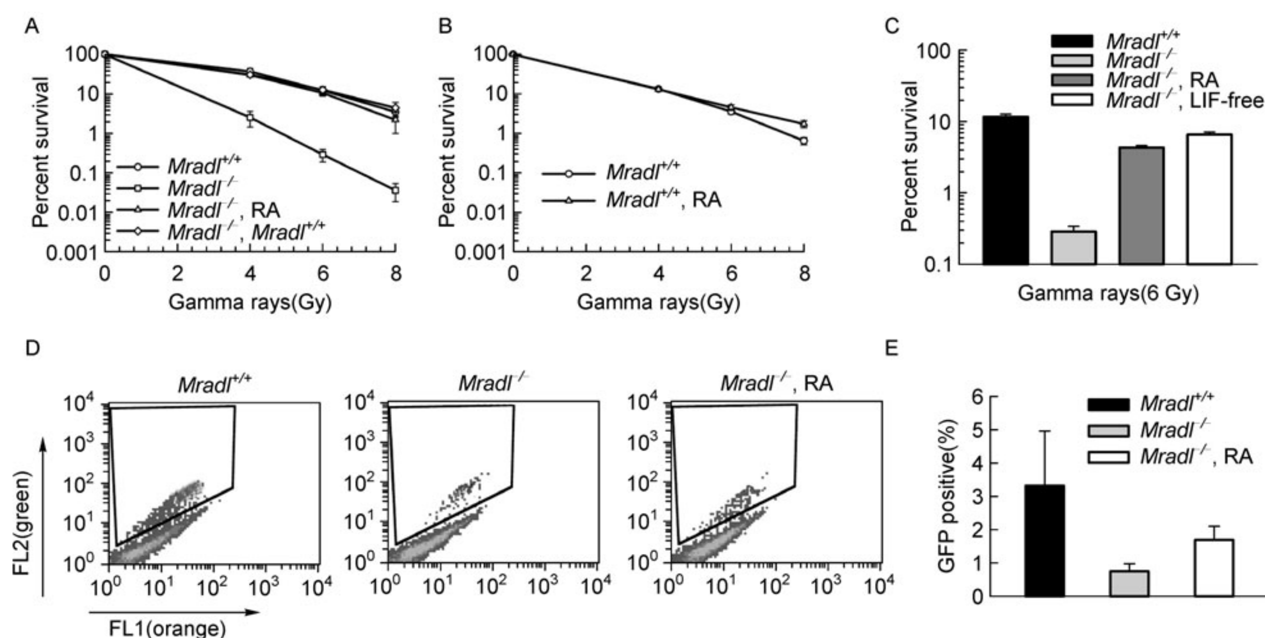

Figure 9. Differentiated *Mrad1*$^{-/-}$ ES cells have increased DSBs repair capability. After treating with gamma rays, enhanced resistance was observed in differentiated *Mrad1*$^{-/-}$ ES cells (A), but not *Mrad1*$^{+/+}$ ES cells (B). Other differentiation-inducing method indicated the same results (C). Points in all the graphs represented the average of three independent experiments with bars indicating standard deviation. Meanwhile, flow cytometric analysis demonstrated attenuated HR in *Mrad1*$^{-/-}$ ES cells, but partial compensation in differentiated *Mrad1*$^{-/-}$ ES cells. ES cells containing a chromosomal DR-GFP reporter were cotransfected with the expression vectors for the I-*Sce*I endonuclease. *In vivo* cleavage of DR-GFP reporter at the I-*Sce*I site of SceGFP gene and repair by the downstream iGFP repeat directed HR resulted in GFP-positive cells (D). Summary of the percentage of HR deficient cells from each cell lines is presented. Bars represent the average of three independently isolated hprtDRGFP subclones for each cell line (E). Error bars are ± S.D. (n = 3).

checkpoint maintenance, but intact in intra-S phase checkpoint, which is in contrast to *Mhus1* embryonic fibroblasts (EF) (Weiss et al., 2000, 2003; Hopkins et al., 2004). Taken together, *Rad1*, *Rad9* and *Hus1* are likely to work in the 9-1-1 complex for the resistance to HU, UV light and gamma rays as well as for the maintenance of S/M and G_2/M checkpoints in mouse ES cells. The phenotype differences in intra-S phase, S/M and G_2/M checkpoints between *Mrad1* or *Mrad9*-deleted mouse ES cells and *Mhus1*-deleted mouse EF cells are probably due to the various differentiation states, suggesting the different functions of these genes in cell cycle checkpoints in ES and EF cells.

Consistent with the above hypothesis, we found in this study that the differentiated *Mrad1*$^{-/-}$ cells induced by RA and LIF-free media had similar resistance to gamma rays as undifferentiated or differentiated *Mrad1*$^{+/+}$ cells (Fig. 9). Interestingly, the resistance to HU or UV light was similar between undifferentiated and differentiated *Mrad1*$^{-/-}$ cells (our unpublished data). These results together suggest that differentiation has various influence on different DNA repair pathways. It is still unknown whether differentiation of *Mrad9*$^{-/-}$ cells can also enhance their resistance to gamma rays. This experiment is critical to clarify whether the differentiation-associated resistance change is 9-1-1 complex dependent or only Rad1-dependent. Indeed, there are significant amounts of individual Rad1 molecules in human cells (Burtelow et al., 2001; our unpublished data).

ES cells were reported to have higher DNA repair abilities than differentiated cells (Maynard et al., 2008; Tichy and Stambrook, 2008). Our results are inconsistent with these reports. It is possible that repair factors work differently at various stages of differentiation, and the comparison between ES and differentiated cells only at certain stages probably does not reflect all the DNA repair situations of mammalian cells during differentiation. In addition, various DNA repair pathways are probably differently influenced by cell differentiation as shown in this study while only the resistance to gamma rays, but not to HU or UV light, was altered by the differentiation of mouse ES cells. As already shown by many studies, differentiation is largely regulated and reflected by chromatin status and many chromatin remodeling factors play important roles in DNA repair pathways. DNA repair at different stages of differentiation attracts more researches and will generate further insights into DNA repair mechanisms.

HR repair was a major component that was altered in DSB

 © Higher Education Press and Springer-Verlag Berlin Heidelberg 2011

repair from mouse ES *Mrad1*$^{-/-}$ cells to RA-induced differentiated mouse *Mrad1*$^{-/-}$ cells (Fig. 9D and 9E), but it only accounted for half of the altered DSB. It is likely that NHEJ also changed during the differentiation. If this is true, the differentiation would modulate the common part(s) of both repair pathways, and the chromatin status during DSB repairing process might be modulated

A study of human HCT116 cells with *RAD1* siRNA demonstrated no effect of the corresponding reduced protein levels on the G_2/M checkpoint, but impaired intra-S phase checkpoint control was observed (Bao et al., 2004). Our study using *Mrad1*-deficient ES cells revealed the opposite results: a defective G_2/M and an intact intra-S phase checkpoint (Fig. 4 and 6). The difference in cell types might contribute to the different checkpoint responses. As for the lack of a role of human *RAD1* in G_2/M checkpoint as shown by knockdown strategy, a possibility also exists that a low level of *RAD1* is sufficient to support G_2/M checkpoint function.

MATERIALS AND METHODS

Growth of ES cells, gene targeting, and generation of *Mrad1*-deficient cells

Mrad1$^{+/-}$ ES cells were prepared as previously described (Han et al., 2010). To generate *Mrad1*$^{-/-}$ ES cells, *Mrad1*$^{+/-}$ ES cells were grown in a medium containing 3.2–4.4 mg/mL G418. For the construction of *Mrad1*$^{-/-}$ ES cells that ectopically express wild-type gene, the cells were transfected with pZeoSV2-*Mrad1*, grown in the presence of zeocin (30 μg/mL), and resistant clones were examined by RT-PCR to identify *Mrad1* transcription.

The *Mrad1* expression vector was made by PCR from mouse cDNA with the primers: 5′-ATTCGGCCGACTCGAGTCAAGACT-CAGGAACTTCTTCATCAG-3′ and 5′-GTCCATAAGCTTGCCGC-CACCATGCCTCTCCTAACCCAGTACAATG-3′. The product was cut with *Xho*I/*Hin*dIII and subcloned into pZeoSV2 (Invitrogen).

Retinoic acid (RA)-induced differentiated ES cells were prepared using normal *Mrad1*$^{+/+}$ and *Mrad1*$^{-/-}$ ES cells cultured in 8 μmol/L RA for 5 days.

Southern blotting and PCR assays to assess genotypes

Genomic DNA was isolated from ES cells and mouse tails using published methods (Weiss et al., 2000). For southern blotting, DNA was digested with *Hin*dIII, separated on a 0.7% agarose gel, then transferred to a nylon membrane, and hybridized to a ^{32}P-labeled probe, which was generated by PCR using primers: 5'-GTGGCCTAGGTGGTTGCGTATCTGAAC-3' and 5'-GTCGGCTCC-GAGAAGAAGGATGCTCC-3' with mouse genomic DNA as template.

To genotype ES cells and mice by PCR, the reaction was performed using genomic DNA templates and the following primer pairs: 5'-GTCTCAGGTTTTCACACATCTTCC-3' and 5'-GCTTA-TATTCTAGAAACCTTCCTGTATG-3'. After denaturation at 94°C for 5 min, 35 cycles of amplification (94°C for 13 s, 59°C for 30 s, at 72°C for 3 min 10 s) were followed, with a final extension at 72°C for 10 min.

Northern blotting and RT-PCR

Total RNA was isolated from ES cells using RNeasy Mini kit (QIAGEN) as described by the manufacturer. For Northern blotting, 10 μg RNA was fractionated in a 1.2% (*w*/*v*) formaldehyde-agarose gel and then transferred to a Hybond-N membrane. Templates for probes were made by PCR using the following primers: *Mhus1*, 5'-ATGAAGTTTCGCGCCAAGAT-3' and 5'-AGTCTGGGATG-GAGGGTTCT-3'; *Mrad9*, 5'-ACTATTGAGGATTCCTTGCTGGATG-3' and 5'-ACAGTGAACGAAACTTCTTGGGTG-3'; *Mrad1*, 5'-GGAGTTTCCTGCATTTCCAAAAG-3' and 5'-GTCCATAAGCTT-CCTCTCCTAACCCAGTACAATGAAGAG-3'; *neo*, 5'-CTACGCGTC-GACATTGAACAAGATGGATTGCACGC-3' and 5'-AGGAATTCAGA-CATGATAAGATACATTGATGAG-3'; *p21*, 5'-ATGTCCAATC-CTGGTGATGTCCG-3' and 5'-CAGGCTGGTCTGCCTCCGTTTTC-3'. Then, the membrane was hybridized with the probes, which were made using [α-32P]-dCTP and the Prime-a-gene labeling system (Amersham). The labeled membrane was washed and used to expose X-ray film.

For RT-PCR, 2 μg total RNA was reverse-transcribed to cDNA using the SuperScript First-Strand Synthesis System for RT-PCR (Invitrogen). PCR amplification was carried out using the following primer pairs: *Mrad1* ORF, 5'-TCCATAAGCTTCCTCTCCTAACCCAG-TACAATGAAGAG-3' and 5'-ACTGCCATAACTCGAGTCAAGACT-CAGGAACTTCTTCATCAGG-3'; *Mrad1* upstream, 5'-ATGCCTCT-CCTAACCCAGTACAATG-3' and 5'-TTCTTCCTGAATGA-CAAATTCCTG-3'; *Gapdh*, 5'- GCAAAGTGGAGATTGTTGCC-3' and 5'-CCGTATTCATTGTCATACCA-3'.

Western blotting

Cell lysate for western blotting was prepared in 1 × SDS-sample buffer, with the final concentration of 10^4 cells/μL. 3 μL lysates were resolved on a 10% SDS-PAGE gel, and proteins were transferred to a polyvinylidene difluoride membrane. The membrane was probed consecutively with primary and peroxidase-conjugated secondary antibodies, and the signal was detected using the SuperSignal West Pico Chemiluminescence Substrate system (Prod #34077, Pierce). Primary and secondary antibodies used in this study were mouse anti-phospho-H2AX (Upstate), mouse anti-tubulin (Sigma), mouse anti-p21 (Santa Cruz), rabbit anti-p53 (Santa Cruz), chicken anti-RAD9, anti-HUS1, peroxidase-conjugated anti-chicken IgY (A9046, Sigma), peroxidase-conjugated anti-mouse IgG (A9044, Sigma), and peroxidase-conjugated anti-rabbit IgG (A9169, Sigma). The anti-RAD9 and anti-HUS1 antibodies were isolated from the eggs of chickens immunized with full-length human RAD9 and HUS1 proteins, respectively.

Cell survival assays

ES cells were plated in duplicate or triplicate and grown for 16 h before treatment. To test hydroxyurea (HU) sensitivity, the drug was added to the medium to achieve the designated final concentrations. After 24 h incubation, cells were washed twice with phosphate-buffered saline (PBS), a fresh medium without HU was added back, and the cells were incubated for 10 more days before Giemsa stain and colony counting. To assess the ionizing radiation sensitivity, cells were exposed to graded doses of gamma rays using a ^{60}Co-based

© Higher Education Press and Springer-Verlag Berlin Heidelberg 2011

irradiator, and incubated for another 10 days to allow colony formation. To determine the sensitivity to 254-nm UV light, the medium was removed, and the cells were exposed to graded doses of the UV light, and then the fresh medium was added to the cells, which were incubated for 10 more days before colony number was assessed. Survival percentage was calculated as 100 × [(number of colonies in treated dishes/number of cells seeded in treated dishes)/(number of colonies in mock-treated control dishes/number of cells seeded in mock-treated control dishes)]. Mean values were derived from three independent replicates, and the standard deviations were calculated.

Assays for cell cycle checkpoint functions

To evaluate G_2/M checkpoint control, 10^6 cells were plated on 10-cm dishes and incubated at 37°C in 5% CO_2 overnight. Two sets of cells were exposed to 10 Gy of gamma rays, with one set mock treated as a control. Immediately after irradiation, colcemid (final concentration of 50 ng/mL) was added to one irradiated set of cells, which were subsequently incubated for various times at 37°C. Cells were processed, stained with propidium iodide (PI) and analyzed by an FACSCalibur flow cytometer (Becton Dickinson) using an established method (Hang and Fox, 2004).

S/M checkpoint function was examined using published procedures (Hu et al., 2008). Briefly, ES cells were grown to 70% confluence, and 1 mmol/L HU was added to the medium to achieve a drug concentration of 1 mmol/L. Cells were incubated at 37°C in 5% CO_2 for various times, processed and suspended in PBS. The cells were probed with rabbit anti-phospho-histone H3 (Upstate), then FITC-conjugated anti-rabbit antibodies (Jackson ImmunoResearch Laboratories, INC), and stained with PI before flow cytometric analysis.

Intra-S phase checkpoint function was also evaluated by radio-resistant DNA synthesis (RDS) assay in the BrdU labeling experiment (Hang and Fox, 2004). Briefly, cells were grown to 70% confluence. The medium was removed and cells were exposed to 20 J/m^2 UV light. Afterwards, pre-warmed medium was added back to dishes, and cells were re-incubated at 37°C. At various times after UV treatment, 10 μmol/L BrdU was added to the medium and cells were pulse-labeled for 10 min. After processed, probed with FITC-conjugated anti-BrdU antibody, and stained with PI, cells were subjected to flow cytometric analysis.

Comet assay

An alkaline comet assay for detecting DNA damage was carried out with the CometAssay kit as described by the manufacturer (TREVIGEN). Briefly, comet assay slides were loaded with a mixture of 10 μL of ES cell suspension (5 × 10^5 cells/mL) and 90 μL of low-temperature melt agarose at a final concentration of 0.75%. After solidification, slides were lysed at 4°C in darkness for 1 h in lysis solution. The slides were soaked and subjected to electrophoresis in alkaline solution, washed and stained with SYBR Green (0.1 μg/mL). The comet images were captured using a fluorescence microscope (Nikon). The tail moment was analyzed using Euclid comet analysis software (Euclid Analysis, St. Louis, MO).

Immunofluorescence assay

Cells grown on coverslips were fixed with 4% paraformaldehyde in PBS for 15 min at room temperature. The coverslips were washed in PBS twice, incubated in PBS containing 0.5% Triton-X100 for 15 min, then in PBS containing 5% BSA and 0.1% Triton-X100 for 1 h, washed in PBS again, and incubated with anti-phospho-H2AX (Upstate) primary antibody (1:100 dilution) in PBS containing 5% BSA and 0.1% Triton-X100 for 1 h at 37°C. Afterwards, coverslips were washed twice for 5 min each in PBS and incubated with FITC-conjugated anti-mouse antibody (1:100 dilution in PBS containing 5% BSA and 0.1% Triton-X100) for 1 h at 37°C. Finally, the coverslips were counterstained with DAPI (10 ng/mL). The images were captured using a fluorescence microscope (Nikon).

Homology-directed recombination assay

ES cell clone with the integrated homologous recombination reporter DR-GFP was generated as described previously (Pierce et al., 2001). 70 μg of the hprtDRGFP plasmid digested with *Kpn*I/*Sac*I was transfected into 2 × 10^7 cells in 0.8 mL of PBS using an electroporator at 800 V and 10 μF. Then cells were plated onto 5 plates, selected by puromycin (1.2 μg/mL) for 7 days and then by 2 μmol/L 6-thioguanine for another 7 days, and the remaining colonies were isolated. The I-*Sce*I expression vector pCBASce was transfected using a Lipofectamine plus protocol. 10^5 ES cells were plated onto a 6-well dish, and transfected with 1 μg I-*Sce*I plasmid using the Lipofectamine plus mixture on the next day. Cells were incubated for 48 h, and then analyzed by FACSCalibur cytometer (Becton Dickinson).

ACKNOWLEDGEMENTS

This work was supported by the National Natural Science Foundation of China (Grant No. 30900813 to ZSH) and the Knowledge Innovation Program of Chinese Academy of Sciences to HH (Grant No. KSCX2-YW-R63).

ABBREVIATIONS

BrdU, bromodeoxyuridine; ES, embryonic stem; DSBs, double-strand breaks; HR, homologous recombination; HU, hydroxyurea; LIF, leukemia inhibitory factor; MEF, mouse embryonic fibroblasts; NHEJ, non-homologous end joining; PI, propidium iodide; RA, retinoic acid; UV, ultraviolet

REFERENCES

al-Khodairy, F., and Carr, A.M. (1992). DNA repair mutants defining G2 checkpoint pathways in Schizosaccharomyces pombe. EMBO J 11, 1343–1350.

Aladjem, M.I., Spike, B.T., Rodewald, L.W., Hope, T.J., Klemm, M., Jaenisch, R., and Wahl, G.M. (1998). ES cells do not activate p53-dependent stress responses and undergo p53-independent apoptosis in response to DNA damage. Curr Biol 8, 145–155.

An, L., Wang, Y., Liu, Y., Yang, X., Liu, C., Hu, Z., He, W., Song, W., and Hang, H. (2010). Rad9 is required for B cell proliferation and immunoglobulin class switch recombination. J Biol Chem 285, 35267–35273.

Bao, S., Lu, T., Wang, X., Zheng, H., Wang, L.E., Wei, Q., Hittelman, W.N., and Li, L. (2004). Disruption of the Rad9/Rad1/Hus1 (9-1-1) complex leads to checkpoint signaling and replication defects. Oncogene 23, 5586–5593.

Bermudez, V.P., Lindsey-Boltz, L.A., Cesare, A.J., Maniwa, Y.,

 © Higher Education Press and Springer-Verlag Berlin Heidelberg 2011

Griffith, J.D., Hurwitz, J., and Sancar, A. (2003). Loading of the human 9-1-1 checkpoint complex onto DNA by the checkpoint clamp loader hRad17-replication factor C complex in vitro. Proc Natl Acad Sci U S A 100, 1633–1638.

Burtelow, M.A., Roos-Mattjus, P.M., Rauen, M., Babendure, J.R., and Karnitz, L.M. (2001). Reconstitution and molecular analysis of the hRad9-hHus1-hRad1 (9-1-1) DNA damage responsive checkpoint complex. J Biol Chem 276, 25903–25909.

Doré, A.S., Kilkenny, M.L., Rzechorzek, N.J., and Pearl, L.H. (2009). Crystal structure of the rad9-rad1-hus1 DNA damage checkpoint complex—implications for clamp loading and regulation. Mol Cell 34, 735–745.

Ellison, V., and Stillman, B. (2003). Biochemical characterization of DNA damage checkpoint complexes: clamp loader and clamp complexes with specificity for 5′ recessed DNA. PLoS Biol 1, E33.

Enoch, T., Carr, A.M., and Nurse, P. (1992). Fission yeast genes involved in coupling mitosis to completion of DNA replication. Genes Dev 6, 2035–2046.

Freire, R., Murguía, J.R., Tarsounas, M., Lowndes, N.F., Moens, P.B., and Jackson, S.P. (1998). Human and mouse homologs of Schizosaccharomyces pombe rad1(+) and Saccharomyces cerevisiae RAD17: linkage to checkpoint control and mammalian meiosis. Genes Dev 12, 2560–2573.

Han, L., Hu, Z., Liu, Y., Wang, X., Hopkins, K.M., Lieberman, H.B., and Hang, H. (2010). Mouse Rad1 deletion enhances susceptibility for skin tumor development. Mol Cancer 9, 67.

Hang, H., and Fox, M.H. (2004). Analysis of the mammalian cell cycle by flow cytometry. Methods Mol Biol 241, 23–35.

Hang, H., and Lieberman, H.B. (2000). Physical interactions among human checkpoint control proteins HUS1p, RAD1p, and RAD9p, and implications for the regulation of cell cycle progression. Genomics 65, 24–33.

Hartwell, L.H., and Weinert, T.A. (1989). Checkpoints: controls that ensure the order of cell cycle events. Science 246, 629–634.

Hopkins, K.M., Auerbach, W., Wang, X.Y., Hande, M.P., Hang, H., Wolgemuth, D.J., Joyner, A.L., and Lieberman, H.B. (2004). Deletion of mouse rad9 causes abnormal cellular responses to DNA damage, genomic instability, and embryonic lethality. Mol Cell Biol 24, 7235–7248.

Hu, Z., Liu, Y., Zhang, C., Zhao, Y., He, W., Han, L., Yang, L., Hopkins, K.M., Yang, X., Lieberman, H.B., *et al.* (2008). Targeted deletion of Rad9 in mouse skin keratinocytes enhances genotoxin-induced tumor development. Cancer Res 68, 5552–5561.

Levitt, P.S., Liu, H., Manning, C., and Weiss, R.S. (2005). Conditional inactivation of the mouse Hus1 cell cycle checkpoint gene. Genomics 86, 212–224.

Levitt, P.S., Zhu, M., Cassano, A., Yazinski, S.A., Liu, H., Darfler, J., Peters, R.M., and Weiss, R.S. (2007). Genome maintenance defects in cultured cells and mice following partial inactivation of the essential cell cycle checkpoint gene Hus1. Mol Cell Biol 27, 2189–2201.

Lieberman, H.B., Hopkins, K.M., Laverty, M., and Chu, H.M. (1992). Molecular cloning and analysis of Schizosaccharomyces pombe rad9, a gene involved in DNA repair and mutagenesis. Mol Gen Genet 232, 367–376.

Lindsey-Boltz, L.A., Bermudez, V.P., Hurwitz, J., and Sancar, A. (2001). Purification and characterization of human DNA damage checkpoint Rad complexes. Proc Natl Acad Sci U S A 98, 11236–11241.

Longhese, M.P., Paciotti, V., Fraschini, R., Zaccarini, R., Plevani, P., and Lucchini, G. (1997). The novel DNA damage checkpoint protein ddc1p is phosphorylated periodically during the cell cycle and in response to DNA damage in budding yeast. EMBO J 16, 5216–5226.

Lydall, D., and Weinert, T. (1997). G2/M checkpoint genes of Saccharomyces cerevisiae: further evidence for roles in DNA replication and/or repair. Mol Gen Genet 256, 638–651.

Maynard, S., Swistowska, A.M., Lee, J.W., Liu, Y., Liu, S.T., Da Cruz, A.B., Rao, M., de Souza-Pinto, N.C., Zeng, X., and Bohr, V.A. (2008). Human embryonic stem cells have enhanced repair of multiple forms of DNA damage. Stem Cells 26, 2266–2274.

Murray, J.M., Carr, A.M., Lehmann, A.R., and Watts, F.Z. (1991). Cloning and characterisation of the rad9 DNA repair gene from Schizosaccharomyces pombe. Nucleic Acids Res 19, 3525–3531.

Parker, A.E., Van de Weyer, I., Laus, M.C., Oostveen, I., Yon, J., Verhasselt, P., and Luyten, W.H. (1998). A human homologue of the Schizosaccharomyces pombe rad1+ checkpoint gene encodes an exonuclease. J Biol Chem 273, 18332–18339.

Parrilla-Castellar, E.R., Arlander, S.J., and Karnitz, L. (2004). Dial 9-1-1 for DNA damage: the Rad9-Hus1-Rad1 (9-1-1) clamp complex. DNA Repair (Amst) 3, 1009–1014.

Paulovich, A.G., and Hartwell, L.H. (1995). A checkpoint regulates the rate of progression through S phase in S. cerevisiae in response to DNA damage. Cell 82, 841–847.

Pierce, A.J., Hu, P., Han, M., Ellis, N., and Jasin, M. (2001). Ku DNA end-binding protein modulates homologous repair of double-strand breaks in mammalian cells. Genes Dev 15, 3237–3242.

Rauen, M., Burtelow, M.A., Dufault, V.M., and Karnitz, L.M. (2000). The human checkpoint protein hRad17 interacts with the PCNA-like proteins hRad1, hHus1, and hRad9. J Biol Chem 275, 29767–29771.

Roos-Mattjus, P., Vroman, B.T., Burtelow, M.A., Rauen, M., Eapen, A. K., and Karnitz, L.M. (2002). Genotoxin-induced Rad9-Hus1-Rad1 (9-1-1) chromatin association is an early checkpoint signaling event. J Biol Chem 277, 43809–43812.

Rowley, R., Subramani, S., and Young, P.G. (1992). Checkpoint controls in Schizosaccharomyces pombe: rad1. EMBO J 11, 1335–1342.

Shiomi, Y., Shinozaki, A., Nakada, D., Sugimoto, K., Usukura, J., Obuse, C., and Tsurimoto, T. (2002). Clamp and clamp loader structures of the human checkpoint protein complexes, Rad9-1-1 and Rad17-RFC. Genes Cells 7, 861–868.

Sohn, S.Y., and Cho, Y. (2009). Crystal structure of the human rad9-hus1-rad1 clamp. J Mol Biol 390, 490–502.

Tichy, E.D., and Stambrook, P.J. (2008). DNA repair in murine embryonic stem cells and differentiated cells. Exp Cell Res 314, 1929–1936.

Udell, C.M., Lee, S.K., and Davey, S. (1998). HRAD1 and MRAD1 encode mammalian homologues of the fission yeast rad1(+) cell cycle checkpoint control gene. Nucleic Acids Res 26, 3971–3976.

Wang, X., Guan, J., Hu, B., Weiss, R.S., Iliakis, G., and Wang, Y. (2004). Involvement of Hus1 in the chain elongation step of DNA replication after exposure to camptothecin or ionizing radiation. Nucleic Acids Res 32, 767–775.

Wang, X., Hu, B., Weiss, R.S., and Wang, Y. (2006). The effect of Hus1 on ionizing radiation sensitivity is associated with homologous recombination repair but is independent of nonhomologous

© Higher Education Press and Springer-Verlag Berlin Heidelberg 2011

end-joining. Oncogene 25, 1980–1983.

Weiss, R.S., Enoch, T., and Leder, P. (2000). Inactivation of mouse Hus1 results in genomic instability and impaired responses to genotoxic stress. Genes Dev 14, 1886–1898.

Weiss, R.S., Leder, P., and Vaziri, C. (2003). Critical role for mouse Hus1 in an S-phase DNA damage cell cycle checkpoint. Mol Cell Biol 23, 791–803.

Xu, M., Bai, L., Gong, Y., Xie, W., Hang, H., and Jiang, T. (2009). Structure and functional implications of the human rad9-hus1-rad1 cell cycle checkpoint complex. J Biol Chem 284, 20457–20461.

Yazinski, S.A., Westcott, P.M., Ong, K., Pinkas, J., Peters, R.M., and Weiss, R.S. (2009). Dual inactivation of Hus1 and p53 in the mouse mammary gland results in accumulation of damaged cells and impaired tissue regeneration. Proc Natl Acad Sci U S A 106, 21282–21287.

Zhou, M., Zheng, L., Guo, L., and Ding, Z. (2010). Cell Biological Effect and Mechanism of Ultraviolet Radiation. Acta Biophysica Sinica 26, 950–958.

 © Higher Education Press and Springer-Verlag Berlin Heidelberg 2011